

# DMTTF-CA revisited: temperature-induced valence and structural instability

Paolo Ranzieri,<sup>1</sup> Matteo Masino,<sup>1</sup> Alberto Girlando,<sup>1</sup> and Marie-Hélène Lemée-Cailleau<sup>2</sup>

<sup>1</sup>*Dip. Chimica Generale ed Inorganica, Chimica Analitica e Chimica Fisica,  
Università di Parma, Parco Area delle Scienze, 43100-I Parma, Italy*

<sup>2</sup>*Institut Laue-Langevin, 38042 Grenoble, France*

We report a detailed spectroscopic investigation of temperature-induced valence and structural instability of the mixed-stack organic charge-transfer (CT) crystal 4,4'-dimethyltetrathiafulvalene-chloranil (DMTTF-CA). DMTTF-CA is a derivative of tetrathiafulvalene-chloranil (TTF-CA), the first CT crystal exhibiting the neutral-ionic transition by lowering temperature. We confirm that DMTTF-CA undergoes a continuous variation of the ionicity on going from room temperature down to  $\sim 20$  K, but remains on the neutral side throughout. The stack dimerization and cell doubling, occurring at 65 K, appear to be the driving forces of the transition and of the valence instability. In a small temperature interval just below the phase transition we detect the coexistence of molecular species with slightly different ionicities. The Peierls mode(s) precursors of the stack dimerization are identified.

## I. INTRODUCTION

Organic charge-transfer (CT) crystals made up by  $\pi$  electron-donor (D) and electron acceptor (A) molecules often exhibit a typical stack structure, with D and A molecules alternating along one direction.<sup>1,2</sup> The quasi-one-dimensional electronic structure is stabilized by the CT interaction between D and A, so that the ground state average charge on the molecular sites, or degree of ionicity,  $\rho$ , assumes values between 0 and 1. Crystals characterized by  $\rho \lesssim 0.5$  are *conventionally* classified as quasi-neutral (N), as opposed to the quasi-ionic (I) ones, with  $\rho \gtrsim 0.5$ . As discussed for the prototypical system of tetrathiafulvalene-chloranil (TTF-CA),<sup>3</sup> a few CT salts have N-I and Peierls transition, in which  $\rho$  changes rapidly and the regular stack dimerizes, yielding a potentially ferroelectric ground state.<sup>4</sup> N-I transitions are valence instabilities implying a *collective* CT between D and A sites, and as such are accompanied by many intriguing phenomena, such as dielectric constant anomalies, current-induced resistance switching, relaxor ferroelectricity, and so on.<sup>5</sup> The isostructural series formed by 4,4'-dimethyltetrathiafulvalene (DMTTF) with substituted CAs, in which one or more chlorine atom is replaced by a bromine atom, is particularly interesting. In this case, in fact, the transition temperature and related anomalies can be lowered towards zero by chemical or physical pressure, attaining the conditions of a quantum phase transition.<sup>6,7,8</sup>

Albeit several aspects of the N-I transition in Br substituted DMTTF-CA family are worth further studies, the motivation of the present work is far more limited, as we want first of all clarify the mechanism of the transition in the pristine compound, DMTTF-CA. Despite intensive studies,<sup>6,7,8,9,10,11</sup> the transition still presents controversial aspects. Through visible reflectance spectra of single crystals and absorption spectra of the powders, Aoki<sup>9</sup> suggested that by lowering the temperature below 65 K, DMTTF-CA does not undergo a full N-I transition, but forms a phase in which both N ( $\rho = 0.3 - 0.4$ ) and I ( $\rho = 0.6 - 0.7$ ) species are present. The struc-

tural investigation as a function of temperature<sup>10</sup> put in evidence a fundamental aspect of the transition, only implicit in Aoki's work:<sup>9</sup> At 65 K the unit cell doubles along the  $c$  axis ( $a$  is the stack axis). The order parameter of the transition, which is second-order, is the cell doubling coupled with the dimerization.<sup>10</sup> So above 65 K the cell contains one stack, and at 40 K contains two stacks, both dimerized, and inequivalent (space group  $P1$ ). From the bond distances,  $\rho$  is estimated at 0.3 and 0.7-0.8 for the two stacks, respectively.<sup>10</sup> In this view, and considering that the two stacks are dimerized in anti-phase, at low temperature DMTTF-CA has a *ferrielectric* ground state.

However, the above scenario has been questioned.<sup>6,7</sup> Polarized single crystal infrared (IR) reflectance measurements suggests that N and I stacks do not coexist. Only one ionicity is observed, changing continuously from about 0.25 at room temperature to about 0.48 at 10 K, the maximum slope in the  $\rho(T)$  occurring around 65 K. The crystal structure at 14 K indicates a  $P1$  space group, with two equivalent, dimerized stacks in the unit cell, and *anti-ferroelectric* ground state.<sup>7</sup> According to this picture, the mechanism of DMTTF-CA phase transition is very similar to the other N-I transitions.<sup>4,5</sup> The Madelung energy change yields an appreciable change of  $\rho$  (about 0.1) within a few degrees of temperature, accompanied by a stack dimerization. The cell doubling appears to be a secondary aspect, whereas the most important feature is the continuous variation of  $\rho$ , as opposed for instance to the discontinuous, first order transition of TTF-CA.<sup>4</sup>

Some questions remain however unanswered in the above picture.<sup>6,7</sup> The transition displays a continuous ionicity change with  $T$ , and consequently one would expect huge anomalies at the transition, whereas for instance the dielectric constant increase at  $T_c$  is less than in the case of TTF-CA.<sup>4,5</sup> Furthermore, what is the driving force of the transition? In TTF-CA, the N-I transition is attributed to the increase of Madelung energy by the lattice contraction.<sup>3</sup> If it is so also for DMTTF-CA, what is the role of cell doubling? Finally, although  $P1$  and

$P\bar{1}$  space groups are sometimes difficult to disentangle by X-ray diffraction, the issue of the different published structures is not solved, both exhibiting good confidence factors in the refinement process<sup>7,10</sup>

In order to clarify these open questions, and to understand the mechanism of the phase transition in DMTTF-CA, we have decided to collect and re-analyze complete polarized IR and Raman spectra of DMTTF-CA single crystals, along the same lines followed for TTF-CA.<sup>12,13,14</sup> Indeed, a careful analysis can give information about  $\rho$ , stack dimerization, and the Peierls mode(s) inducing it. Vibrational spectra give information about the *local* structure, and from this point of view are complementary to the X-ray analysis, which probes long range order. We shall show that DMTTF-CA transition can hardly be classified as a N-I transition, the most important aspect being the stack dimerization and cell doubling. We shall also offer some clues about the origin of the discrepancies in the two X-ray determinations.<sup>7,10</sup>

## II. EXPERIMENTAL

DMTTF-CA single crystals have been prepared as previously described.<sup>10</sup> The IR spectra (600-8000  $\text{cm}^{-1}$ ) have been obtained with a Bruker IFS66 FTIR spectrometer, equipped with A590 microscope. Raman spectra have been recorded with a Renishaw 1000 micro-spectrometer. The excitation of Raman has been achieved with a Lexel Krypton laser ( $\lambda = 647.1 \text{ nm}$ ), backscattering geometry, with less than 1 mW power to avoid sample heating. A pre-monochromator has been used for the low-frequency spectra (below 200  $\text{cm}^{-1}$ ). For the high frequency Raman spectra we report only the spectra obtained for incident and scattered light both polarized perpendicularly to the stack axis, ( $\perp\perp$ ) in the conventional notation. In this arrangement the in-plane molecular modes, notably the totally symmetric ones, are more clearly visible. The spectral resolution of IR and Raman spectra is 2  $\text{cm}^{-1}$ .

Temperatures down to 10 K have been reached with a ARS closed-circle cryostat, fitted under the IR and Raman microscopes. The temperature reading on the cold finger has been tested and considered accurate to  $\pm 2 \text{ K}$  for the Raman and IR reflectance measurement, where silver paste has been used to glue the sample to the cold finger. For IR absorption the temperature reading is far less accurate, due to the imperfect thermal contact between the sample and the KBr window on the cold finger. Temperature reading corrections have been applied based on the comparison with the reflectivity data. DMTTF-CA reflectivity has been normalized to that of an Al mirror, without further corrections. Therefore the reflectance values are not absolute, and relative values can be compared with confidence only within each low-temperature run. We consider reflectance values of the spectra below 20 K not reliable in any case, because the deposition of an unknown contaminant on the DMTTF-CA surface introduces high noise above  $\sim 2000 \text{ cm}^{-1}$ .

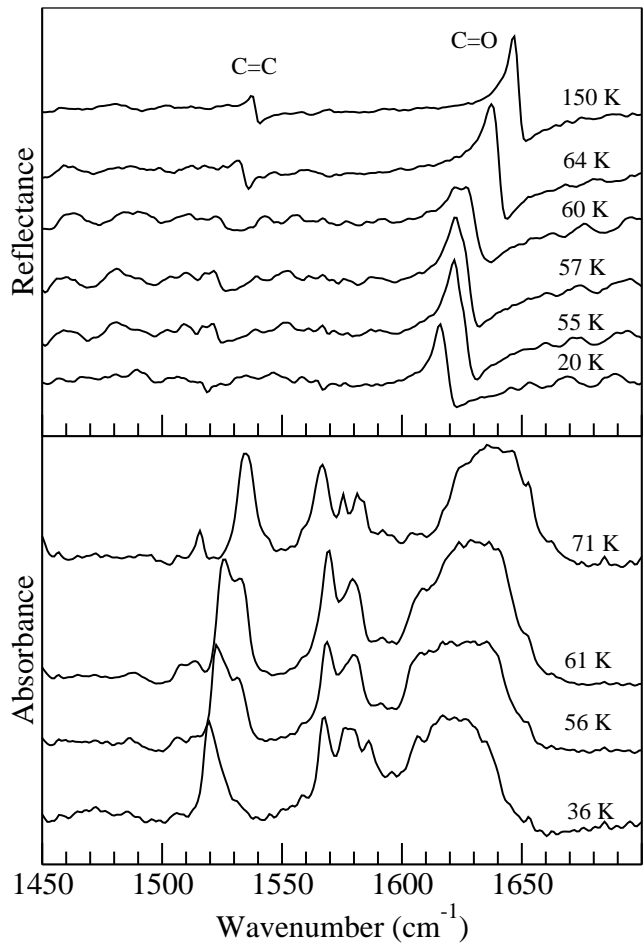


FIG. 1: Temperature evolution of DMTTF-CA reflectance and absorbance spectra, polarized perpendicularly to the stack. The bands corresponding to C=O and C=C stretchings of CA are marked.

## III. RESULTS

### A. Valence instability

The first question we address is that of the ionicity as a function of temperature. To such aim, we have collected both IR reflectance and absorbance spectra, with polarization perpendicular to the stack axis. The two types of spectra allow us to ascertain whether probing the surface or the bulk yields the same result. Unfortunately, we were unable to obtain crystals sufficiently thin to avoid saturation of the most intense absorption bands, so the information provided by the two types of spectra are complementary. Fig. 1 shows some examples of spectra as a function of temperature in the frequency range 1500-1700  $\text{cm}^{-1}$ . The two structures at 1649  $\text{cm}^{-1}$  and 1539  $\text{cm}^{-1}$  (at 150 K) are assigned to the  $b_{1u}\nu_{10}$  and  $b_{2u}\nu_{18}$  modes of the CA moiety, corresponding to the C=O and C=C antisymmetric stretching vibrations, respectively.<sup>12</sup>

The C=O stretching mode is the most sensitive to the molecular charge, so it has been almost invariably used to estimate the ionicity. However, recent investigations on CA and CA<sup>-</sup> molecular vibrations have shown that also the C=C mode should be a good  $\rho$  indicator.<sup>15,16</sup> Therefore we shall use C=O  $b_{1u}\nu_{10}$  as a primary  $\rho$  indicator, and C=C  $b_{2u}\nu_{18}$  mode as secondary, internal consistency probe.

As the C=O stretching mode saturates in absorption (Fig. 1, bottom panel), we have performed the usual Kramers-Kronig transformation of the reflectance spectra. From the frequency reading of the C=O  $b_{1u}\nu_{10}$  mode we have estimated the ionicity by the usual relationship:  $\rho = [\bar{\nu}(0) - \bar{\nu}(\rho)]/\Delta_{ion}$  where  $\bar{\nu}(0)$  is the C=O stretching frequency of the neutral molecule and  $\Delta_{ion}$  is the ionization frequency shift.<sup>12</sup> The resulting  $\rho(T)$  is reported in the top panel of Fig. 2.

The top panel of Fig. 2 is rather similar to the corresponding one of Ref. 6. Indeed, our spectra (Fig. 1) do not show the onset of a strong band around 1580 cm<sup>-1</sup> below 65 K, that according to Aoki *et al.*<sup>9</sup> signals the presence of  $\rho \sim 0.7$  species. Following Ref. 6, we attribute the band around 1580 cm<sup>-1</sup> to an activated  $a_g$  mode, present in the spectra polarized parallel to the stack (see Section III B). However, our data show two significant differences compared with Horiuchi *et al.* results.<sup>6</sup>

First of all, our  $\rho(T)$  curve is consistently shifted downward by about 0.05  $\rho$  units with respect to the corresponding one of Ref. 6. As a consequence, the maximum ionicity at the lowest temperature is well below the N-I borderline, namely 0.43 instead of 0.48. We believe the discrepancy is due to the extrapolation involved in the Kramers-Kronig transformation from reflectance to conductivity. We have indeed verified that different extrapolation procedures may yield different frequencies, and we have chosen extrapolation parameters giving conductivity spectra with frequencies matching those read in absorption (bottom panel of Fig. 1). Our datum is also in agreement with what reported by Aoki,<sup>9</sup> who assigned a  $\rho$  value of  $\sim 0.3 - 0.4$  to the N species at 20 K (although, as stated above, we do not see the insurgence of bands due to I species).

The second important difference of our results compared with those of Horiuchi *et al.*<sup>6</sup> is that just below the phase transition temperature, between 62 and 54 K, the C=O stretching mode shows a clear doublet structure (Fig. 1, top panel), suggesting the presence of two slightly differently charged molecular species. The indication is confirmed by the band due to the C=C stretching mode, which also shows a doublet structure, clearly seen in absorption (bottom panel of Fig. 1). The frequency (and ionicity) difference is small, but clearly visible irrespectively of the direction of temperature change, and reproducible in different runs. Actually, a hint of a doublet structure is visible also in Ref. 6 spectra, but it was interpreted as a band broadening. In Fig. 1 the dashed area indicates the temperature interval of this co-

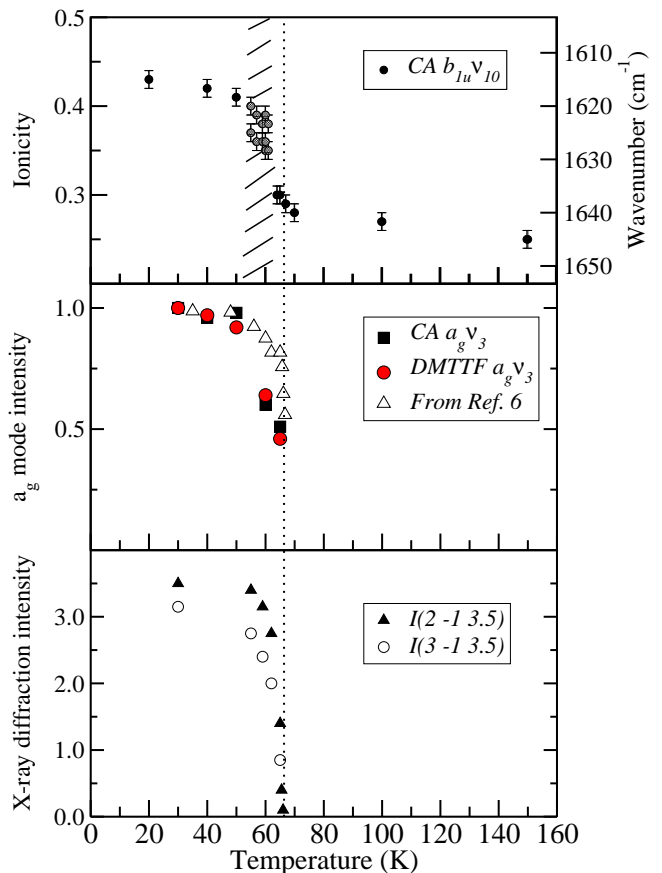


FIG. 2: Temperature evolution of three DMTTF-CA observables. Top panel: Ionicity  $\rho$ . Middle Panel: Normalized intensity of IR vibronic bands, connected to the stack dimerization amplitude. Bottom panel: Intensity of X-ray reflections signaling the cell doubling (from Ref. 10). The vertical dashed line marks the critical temperature  $T_c \simeq 65$  K.

existence.

To summarize, our results present a valence instability scenario different from both the previously reported ones.<sup>6,9</sup> The ionicity change appears to be continuous across the phase transition. The crystal remains neutral ( $\rho \sim 0.43$  at 20 K), therefore excluding the simple term of N-I transition: it is better to refer to it as a valence instability. Finally, in a temperature interval of less than 10 K below 65 K there is coexistence of two species with slightly different molecular ionicity, both on the neutral side, with  $\rho \sim 0.36$  and  $0.38$ .

## B. Dimerization instability

It is well known that IR spectra polarized along the stack are sensible to the symmetry breaking associated with stack distortions. In fact, the loss of inversion center on the molecular units makes the Raman-active totally-symmetric ( $a_g$ ) molecular modes also IR active, with

huge intensity due to their coupling with the CT electronic transition (IR “vibronic bands”).<sup>12</sup> In addition, it has been recently shown that the IR spectra polarized parallel to the stack, associated with Raman, also yield information about pre-transitional phenomena, like the softening of the phonons inducing the stack distortion.<sup>13</sup> To investigate these aspects of the DMTTF-CA phase transition, we have collected the IR reflection spectra polarized parallel to the stack axis. Fig. 3 shows some

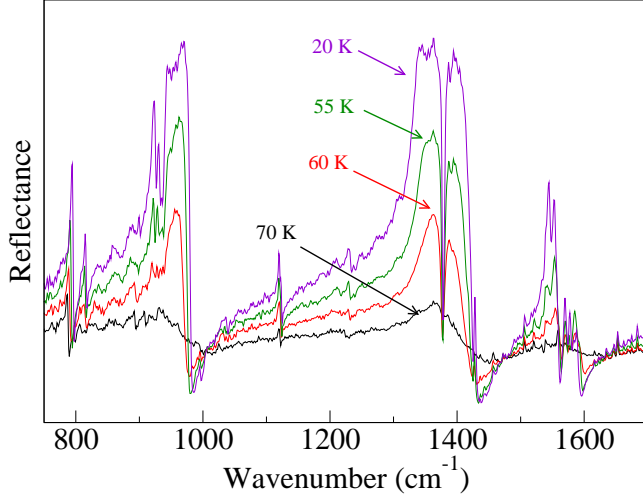


FIG. 3: Temperature dependence of DMTTF-CA reflectance spectra polarized along the stack. The reflectance scale is not reported, as only relative reflectance values can be trusted (see Experimental).

strong features below  $T_c$ . The spectra are identical to those of Ref. 6, and we follow a similar analysis. We focus the attention on the two main features around 1400 and 980  $\text{cm}^{-1}$ , associated with the  $a_g\nu_3$  mode of the TTF skeleton in the DMTTF moiety, and to the  $a_g\nu_3$  mode of CA, respectively.<sup>12</sup> Their intensity  $f_j$  as a function of  $T$  is extracted by fitting the reflectance spectra with a Drude-Lorentz oscillator model, where the dielectric constant is given by:

$$\epsilon(\omega) = \epsilon_\infty + \sum_j \frac{f_j}{\omega_j^2 - \omega^2 - i\omega\gamma_j} \quad (1)$$

In this equation  $\epsilon_\infty$  is the high-frequency dielectric constant, and  $\gamma_j$  is the line width. Now,  $f_j$  is related to  $\delta$ , the dimerization amplitude.<sup>17</sup> The relationship is not of direct proportionality, but in any case  $f_j$  gives an indication of the increase of the dimerization amplitude at the transition.<sup>17</sup> The  $f_j(T)$  for the two modes, normalized at the lowest temperature value (20 K), are reported in the middle panel of Fig. 2 for temperatures below 65 K. Indeed, around the critical temperature one cannot disentangle the contribution to the intensity coming from

the combination modes, as discussed in detail in the next Section. In the same panel we report, for comparison, the normalized intensity relevant to the DMTTF  $a_g$  mode, as given in Ref. 6 for the same temperature range.

The middle panel of Fig. 2 shows that the IR oscillator strengths, related to the stack dimerization amplitude  $\delta$ ,<sup>17</sup> display a behavior typical of an order parameter relevant to a second-order phase transition. It is instructive from this point of view to compare the present data with the intensity of the X-ray diffraction spots related to the cell doubling, as reported in Ref. 10 and shown in the bottom panel of Fig. 2. The two sets of data exhibit the same behavior, demonstrating that the cell doubling, as detected by X-ray, and stack dimerization amplitude, as detected by IR, occur at the same time, representing two inseparable aspects of DMTTF-CA phase transition. On the other hand, the comparison of the three panels in Fig. 2 puts in evidence that the valence instability actually *follows* the structural modification. Dimerization and cell doubling start at  $T_c \simeq 65$  K, whereas the rapid increase in  $\rho$  occurs slightly below, and implies the simultaneous presence of species with two slightly different ionicities in a  $T$  interval of about 10 degrees.

### C. Lattice phonons

If DMTTF-CA phase transition is displacive, it should imply the occurrence of soft phonon(s) yielding the stack dimerization and the cell doubling. In a simplified but effective view, we can think of the phase transition as due to just one critical phonon, with wavevector  $c^*/2$ . Such a phonon belongs to a phonon branch that corresponds to stack dimerization along the  $a$  crystal axis, and at the zone-center is optically active. The driving force of the transition is then provided by the Peierls mechanism, which couples the zone-center dimerization mode, i.e., the Peierls mode, with the CT electronic structure.<sup>18</sup> The electron-phonon causes the softening of the Peierls mode, eventually leading to stack dimerization. However, in the proximity of the phase transition, where interstack interactions are more effective,<sup>11</sup> the Peierls mode evolves to a stack dimerization out-of-phase in nearest-neighbors cells, when it softens yielding the cell doubling along the crystallographic direction  $c$ . Of course, in the complicated phonon structure of a molecular crystal like DMTTF-CA, the Peierls mode may result from the superposition (mixing) of several phonons, all directed along the stack. A spectroscopic investigation of DMTTF-CA, along the lines already developed for TTF-CA,<sup>13,14</sup> should yield the identification of these phonons or of the resulting “effective” Peierls mode.

Phonons coupled to the CT electrons along the chain are most likely inter-molecular, or lattice, phonons.<sup>14</sup> We start by classifying the lattice phonons and their Raman and IR activity by adopting the rigid molecule approximation. This approximation is known to be not fully valid for TTF-CA,<sup>14</sup> but is the only reasonable starting

point in the lack of explicit calculations of DMTTF-CA phonon dynamics. Then, in the high temperature (HT) phase ( $P\bar{1}$ ,  $Z = 1$ )<sup>10</sup> we expect 9 optically active lattice modes,  $6A_g(\mathcal{R}) + 3A_u(\mathcal{T})$ . The Raman active  $A_g$  modes can be described as molecular librations ( $\mathcal{R}$ ), and are decoupled from the CT electrons. Coupling is instead possible for the IR active  $A_u$  phonons, which indeed correspond to translations ( $\mathcal{T}$ ). There are no symmetry constraint about the direction of molecular displacements, so we may have some component of all the three  $A_u$  phonons along the stack axis, contributing to the Peierls mode.

In the low-temperature (LT) phase it is not clear if the two stacks inside the unit cell are inequivalent, with space group  $P1$ ,<sup>10</sup> or equivalent, with space group  $P\bar{1}$ .<sup>7</sup> Since in any case the inequivalence is small, for the spectral predictions we find more convenient to use the centrosymmetric description. The center of inversion is between the two stacks in the unit cell, then we expect 21 optically active modes,  $12A_g(6\mathcal{T} + 6\mathcal{R})$  and  $9A_u(6\mathcal{R} + 3\mathcal{T})$ . Therefore, the phonons modulating the CT integral are IR active in both HT and LT phases, whereas the cell doubling in the LT phase makes Raman active 6 translational phonons, which correspond to the coupled in-phase displacements of the two chains.

Direct investigation of Peierls coupled modes in the far-IR ( $5\text{--}200\text{ cm}^{-1}$ ) is not an easy task.<sup>14</sup> However, in the case of TTF-CA it has been shown<sup>13</sup> that useful information can be obtained from the comparison between Raman and IR spectra polarized parallel to the stack, in the frequency region of molecular vibrations. We have then performed the Kramers-Kronig transformation of the reflectivity data of Section IIIB (Fig. 3), obtaining the optical conductivity spectra which are compared with Raman in Fig. 4.

We again focus attention on the  $a_g\nu_3$  mode of the TTF skeleton in the DMTTF moiety and to the  $a_g\nu_3$  mode of CA, which correspond to the two most prominent Raman bands of Fig. 4, located around  $1400\text{ cm}^{-1}$  and  $980\text{ cm}^{-1}$ , respectively.<sup>12</sup> The IR spectra above 80 K exhibit pairs of absorptions (“side-bands”), symmetrically located above and below the just mentioned Raman bands. The side-bands are quite naturally interpreted as sum and difference combination bands between the corresponding  $a_g$  mode and a lattice phonon.<sup>13</sup> By lowering temperature the side-bands approach each other, and around 80 K they start to coalesce and to overlap to the central Raman band. On the other hand, below the transition temperature (for instance, 60 K in Fig. 4) there is coincidence between Raman and IR bands. As discussed in Section IIIB, both are indeed due to the same  $a_g$  molecular vibration, active in both type of spectra due to the symmetry breaking connected to the stack dimerization.

Analysis of the side-bands therefore gives information on the Peierls mode in the HT phase.<sup>13</sup> In the top panel of Fig. 5 the frequency difference between the DMTTF  $a_g\nu_3$  Raman band and the corresponding IR side-bands is plotted as a function of temperature. We also plot the frequency semi-difference between the side-bands as-

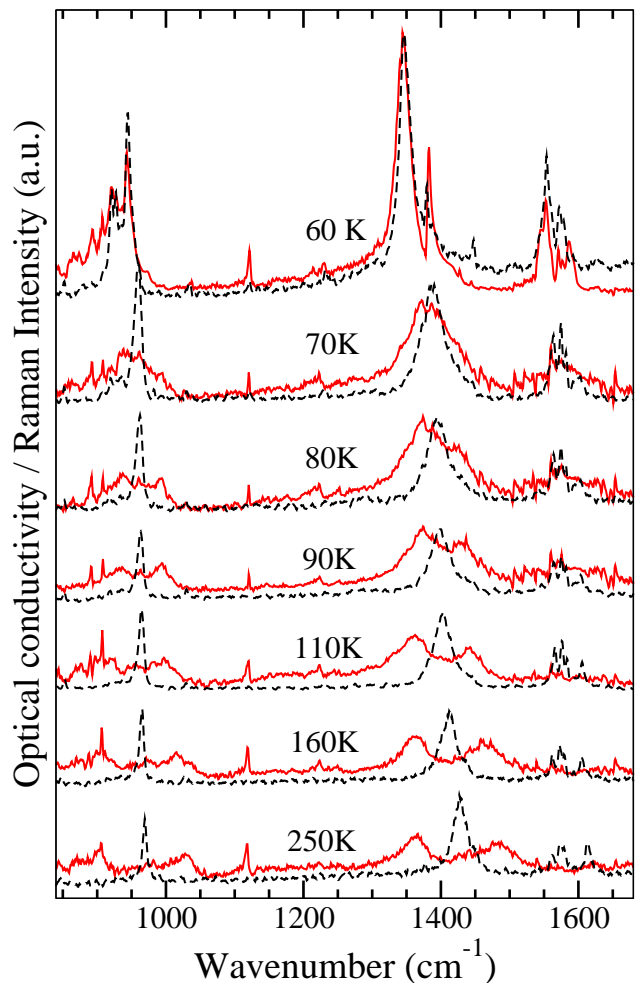


FIG. 4: Temperature dependence of DMTTF-CA Raman spectra (black, dashed line), and IR conductivity spectra polarized parallel to the stack axis (red, continuous line)

sociated with both DMTTF and CA  $a_g\nu_3$  modes. Fig. 5 shows that the data points coincide within experimental error, supporting the idea that *the same* lattice mode is involved in the combination, and clearly indicates a soft mode behaviour. This softening suggests that this lattice phonon is indeed the Peierls mode, or to be precise, the “effective” Peierls mode, resulting from the superposition of several modes coupled to the CT. We cannot follow the frequency evolution down to the transition temperature, since below 80-75 K it becomes impossible to separate the contribution of the two side-bands, letting aside the interference from the fluctuations occurring near the phase transition.

We now turn attention to DMTTF-CA LT phase, where the Peierls mode(s) are active in Raman in addition to IR. We have then measured the Raman spectra in the low-frequency region in order to identify the possible soft phonons. Low-frequency Raman also gives indications about the cell doubling, given the difference in the

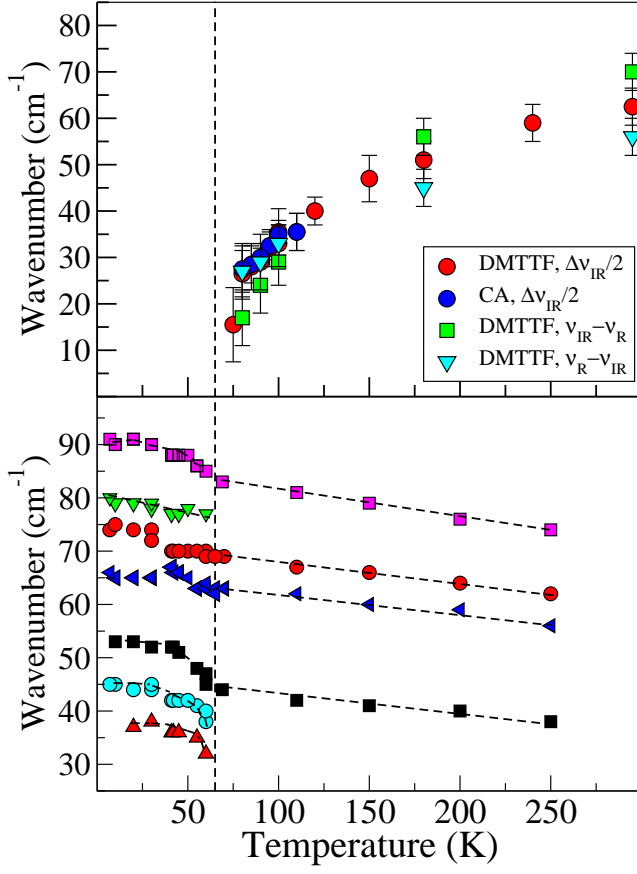


FIG. 5: Top panel: Frequency difference between Raman DMTTF  $a_g\nu_3$  and CA  $a_g\nu_3$  bands and the corresponding IR sidebands of Fig. 4 as a function of temperature. Bottom panel: Temperature evolution of the most intense low-frequency Raman bands. The vertical dashed line marks the critical temperature.

number of phonons present in the two phases.

An example of the low-frequency Raman spectra above and below the phase transition is shown Fig. 6. We report the spectra with two polarizations. In one, both incident and scattered light are polarized perpendicularly to the stack axis ( $\perp\perp$  spectra). In the other, the polarization of the incident light is rotated parallel to the stack axis, the polarization of the scattered light being kept perpendicular to it ( $\parallel\perp$  spectra). The list of the observed bands in both polarizations is reported in Table I. The number of observed phonon modes is less than predicted by the selection rules, but in any case the phonons detected in the HT phase are about a half of those detected at LT, an obvious consequence of cell doubling. The temperature dependence of the Raman frequencies are shown in the bottom panel of Fig. 5. One immediately notice the usual softening for all the modes as we increase the temperature, due to lattice expansion. However, in the LT phase the softening of some phonons is more pronounced close to the critical temperature. The frequency lowering is

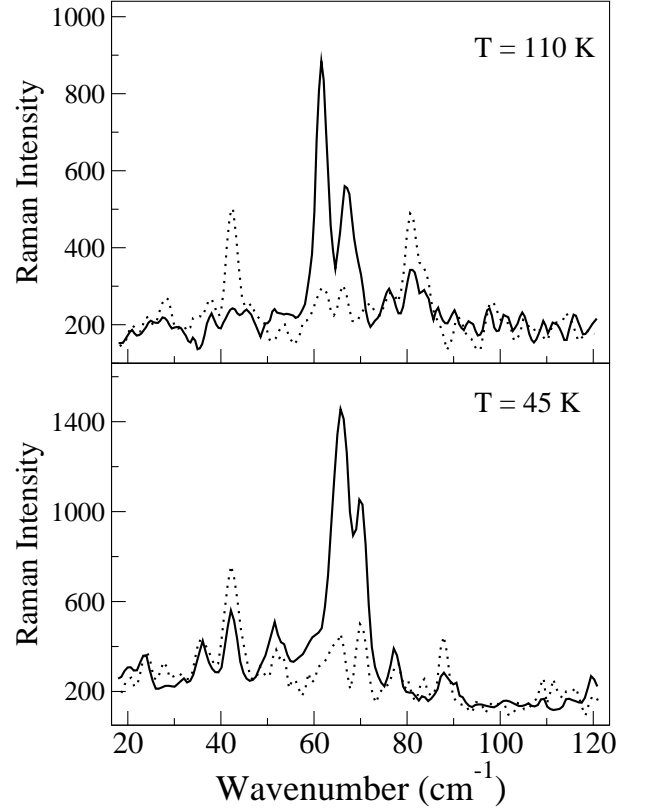


FIG. 6: Top panel: polarized low-frequency Raman spectra of DMTTF-CA at 110 K (HT phase). Bottom panel: polarized low-frequency Raman spectra of DMTTF-CA at 45 K (LT phase). Continuous line indicates ( $\perp\perp$ ) polarization; dashed line ( $\parallel\perp$ ) polarization (see text).

TABLE I. DMTTF-CA Raman active lattice modes in the LT and HT phases.

Mode no.	Raman, 45 K	Raman, 110 K
$\nu_1$	36 ( $\parallel\perp$ )	—
$\nu_2$	42 ( $\parallel\perp$ )	42 ( $\parallel\perp$ )
$\nu_3$	52 ( $\perp\perp$ )	—
$\nu_4$	66 ( $\perp\perp$ )	62 ( $\perp\perp$ )
$\nu_5$	70 ( $\perp\perp$ )	67 ( $\perp\perp$ )
$\nu_6$	77 ( $\perp\perp$ )	—
$\nu_7$	88 ( $\parallel\perp$ )	82 ( $\parallel\perp$ )

not as large as in the HT phase (top panel of Fig. 5), but is certainly present. The relative weakness of the effect compared to the HT phase can be explained considering that in the HT phase we observe the softening of an “effective” Peierls mode, superposition of several phonons all coupled to the CT electrons. In the LT phase, on the other hand, the softening is distributed on several modes, and the phonon description and mixing changes as we approach the phase transition. The effect is clearly seen in Fig. 5, where at about 40 K there is a case of avoided

crossing of two phonons located around  $70 \text{ cm}^{-1}$ . In addition, we have to keep in mind that the DMTTF-CA transition is second order, but cannot be considered a strictly one-dimensional Peierls transition, as the transition implies a change in the number of stacks per unit cell. The actual phase transition mechanism is a complex one, as shown by the fact that just below  $T_c$  there is coexistence of two slightly different degrees of ionicity on the molecular sites (Section III A). This finding might be explained in terms of an inequivalence of the two stacks inside the unit cell in proximity of  $T_c$ .

#### IV. DISCUSSION AND CONCLUSIONS

The present work does not allow us to draw definitive conclusions about the equivalence/inequivalence of the two DMTTF-CA stacks inside the unit cell of the LT phase (anti-ferroelectric or ferroelectric arrangement). As just discussed, the presence of two slightly different degrees of ionicity may imply that just after the phase transition we have a temperature interval ( $\sim 62 - 54 \text{ K}$ ) in which the two stacks are inequivalent with the  $P1$  structure,<sup>10</sup> followed by a definitive structural rearrangement yielding to the  $14 \text{ K } P\bar{1}$  structure.<sup>7</sup> This picture would support the  $P1$  structural determination,<sup>10</sup> collected at  $40 \text{ K}$  below our coexistence  $T$  region, only assuming that the  $P1$  structure refers to a non-equilibrium phase. Such “freezing” of a metastable phase may be a consequence of a too fast sample cooling, a case not uncommon in organic solid state, although most of the times refers to some disordered, glassy phase.<sup>19</sup>

At this point we wish to underline that inequivalence of the stacks does not necessarily imply an appreciably different degree of ionicity. DFT calculations made for the  $P1$  structure at  $40 \text{ K}$  indeed found practically identical  $\rho$  for the two stacks with different dimerization amplitudes.<sup>20</sup> We may then have a scenario with two (slightly) inequivalent stacks, but practically identical  $\rho$ .

IR spectra polarized parallel to the stack (Fig. 3) of course cannot disentangle dimerization amplitudes on different stacks. Optical spectroscopy selection rules, on the other hand, are based on the factor group (unit cell group), therefore reflecting the translational long-range order of the crystal.<sup>21</sup> From this perspective, two findings are in favor of inequivalent stacks, down to at least  $20 \text{ K}$ . The first fact refers to the Raman-IR coincidence observed for the  $a_g$  molecular modes in the LT phase (Fig. 4). If the two stacks are equivalent, and connected by an inversion center, each  $a_g$  mode of one stack would be coupled in-phase and out-of-phase with the same mode on the other stack. The in-phase mode is Raman active, and the out-of-phase one IR active, therefore we should not observe precise frequency coincidence, the difference being related to the strength of inter-stack interaction. Unfortunately, our data are not conclusive in this respect, due to the frequency uncertainties associated with the Kramers-Kronig transformation.<sup>22</sup>

The other experimental observation that can be explained in terms of inequivalent stacks is the doubling of localized electronic transitions below  $65 \text{ K}$ .<sup>9</sup> This experimental observation was the first one that induced Aoki *et al.*<sup>9</sup> to suggest the coexistence of neutral and ionic species, but since then it has been almost forgotten. Horiuchi *et al.*,<sup>6</sup> as well as the present measurements, exclude such coexistence, and the only explanation we can think of the doubling is in term of ordinary Davydov splitting.<sup>21</sup> However, the two components of the Davydov splitting can be both optically active only in the lack of inversion center relating the two stacks, otherwise the *gerade* component is inactive.

Only the replica of structural measurements and/or of the refinement process starting from the two different hypothesis will definitely settle the question of equivalence-inequivalence of DMTTF-CA stacks. On the other hand, this question is not particularly relevant as far as the mechanism of DMTTF-CA phase transition is concerned. The present analysis departs from the previous ones<sup>6,7,8</sup> only in some seemingly marginal details, but actually the resulting picture of the phase transition is completely different.

First of all, we have ascertained that the phase transition implies only a limited change of  $\rho$ , DMTTF-CA remaining on the *neutral* side down to the lowest temperature. Furthermore, the major charge rearrangement *follows*, by a few degrees K, the onset of cell doubling and stack dimerization. The latter finding can be well appreciated from Fig. 2, where the inflection of the  $\rho(T)$  curve occurs around  $61 \text{ K}$ , rather than at  $65 \text{ K}$  for the symmetry breaking. Close scrutiny of Fig. 5 of Ref. 6 conveys the same information. Therefore the transition can hardly be termed N-I, since cell doubling and stack dimerization clearly constitute the driving force of the transition. Indeed, we can envision a scenario in which the dimerization and cell doubling lead to a better molecular packing, with an increase in the Madelung energy and consequent small, continuous change in  $\rho$ . The presence of slightly differently charged molecular species before the dimerization/cell doubling has reached completion (Fig. 2) fits quite naturally into this picture.

Disentangling the contribution of the cell doubling from that of the stack dimerization is a useless endeavor. In any case, our measurements have clearly evidenced the presence of an effective soft mode along the chain (Fig. 5, top panel), so a Peierls-like mechanism is certainly at work in the precursor regime of the phase transition. X-ray diffuse scattering also reveals the importance of electron-phonon coupling along the chain, and of one-dimensional correlations. It has been interpreted in terms of lattice relaxed exciton strings (LR-CT) rather than in terms of a soft mode. The phase transition is then regarded more as a disorder-order transition (ordering of LR-CT exciton strings along and across the chains), and not as a displacive one, with progressive uniform softening of the Peierls mode up to the final chain dimerization. It would be interesting to re-analyze the X-ray

diffuse scattering data to examine whether and to what extent they are compatible with the soft-mode picture. The present results of course only evidence the soft-mode mechanism, and the presence of LR-CT exciton strings cannot be excluded, in particular close to  $T_c$ , in the region where our data cannot be unambiguously interpreted.

The LR-CT exciton string picture has been invoked mainly to account for the dielectric constant anomaly at  $T_c$ , attributed to the progressive ordering of the a paraelectric phase before reaching anti-ferroelectric (or ferroelectric) ordering.<sup>7,11</sup> On the other hand, it has been shown that the Peierls mechanism is also able to *quantitatively* explain the experimental increase of the dielectric constant at  $T_c$ , interpreted as due to charge oscillations induced by the Peierls mode.<sup>18</sup> We underline in this respect that although the dimerization of the stack in the I phase has been often attributed to a spin-Peierls mechanism,<sup>5</sup> the electronic degrees of freedom are involved as well, particularly in proximity of the N-I borderline.<sup>18</sup> In addition, the dimerization transition

may occur also on the N side, provided the electron-phonon interaction is strong enough. This is just the present case, and correspondingly we have an increase of the dielectric constant less important than in the case of TTF-CA,<sup>4,5</sup> as predicted by the calculations.<sup>18</sup> In summary, the present interpretation stresses the importance of the lattice instability over that of charge instability in DMTTF-CA and related compounds.

## V. ACKNOWLEDGMENTS

We gratefully thank N. Karl for providing the DMTTF-CA crystals. The reflectivity data have been fitted by the freely available RefFit program ([optics.unige.ch/alexey/reffitt.html](http://optics.unige.ch/alexey/reffitt.html)). We thank A. Painelli for many useful discussions. Work in Italy supported by the “Ministero dell’Università e Ricerca” (MUR), through FIRB-RBNE01P4JF and PRIN2004033197\_002.

- 
- <sup>1</sup> F. H. Herbestein, in *Perspectives in Structural Chemistry* Vol. IV, J. D. Dunitz and J. A. Ibers Eds., Wiley, New York, 1971, Vol. IV, p. 166.
  - <sup>2</sup> Z.G. Soos, D.J. Klein, in *Treatise on Solid-State Chemistry*, vol. III, N. B. Annay Ed., Plenum Press, New York, 1976, p. 689.
  - <sup>3</sup> J.B. Torrance, J.E. Vasquez, J.J. Mayerle, V.Y. Lee, Phys. Rev. Lett. **46**, 253 (1981); J.B. Torrance, A. Girlando, J.J. Mayerle, J.I. Crowley, V.Y. Lee, P. Batail, S.J. LaPaca, Phys. Rev. Lett. **47**, 1747 (1981).
  - <sup>4</sup> A. Girlando, A. Painelli, S. A. Bewick, Z. G. Soos, Synth. Metals **141**, 129 (2004), and references therein.
  - <sup>5</sup> S. Horiuchi, R. Kumai, Y. Okimoto, Y. Tokura, Chem. Phys. **325**, 78 (2006); S. Horiuchi, T. Hasegawa, Y. Tokura, J. Phys. Soc. Japan **75**, 051016 (2006).
  - <sup>6</sup> S. Horiuchi, Y. Okimoto, R. Kumai, Y. Tokura, J. Am. Chem. Soc. **123** (2001) 665.
  - <sup>7</sup> S. Horiuchi, Y. Okimoto, R. Kumai, Y. Tokura, Science **299**, 229 (2003).
  - <sup>8</sup> Y. Okimoto, R. Kumai, S. Horiuchi, H. Okamoto, Y. Tokura, J. Phys. Soc. Japan, **74**, 2165 (2005).
  - <sup>9</sup> S. Aoki, T. Nakayama, A. Miura, Phys. Rev. B **48**, 626 (1993)
  - <sup>10</sup> E. Collet, M. Buron-Le Cointe, M. H. Lemée-Cailleau, H. Cailleau, L. Toupet, M. Meven, S. Mattauch, G. Heger, N. Karl, Phys. Rev. B **63** 054105 (2001).
  - <sup>11</sup> E. Collet, M. H. Lemée-Cailleau, M. Buron-Le Cointe, H. Cailleau, S. Ravy, T. Luty, J. F. Bérar, P. Czarnecki, N. Karl, Europhys. Lett., **57**, 67 (2002).
  - <sup>12</sup> A. Girlando, F. Marzola, C. Pecile, J.B. Torrance, J. Chem. Phys. **79** 1075 (1983).
  - <sup>13</sup> M. Masino, A. Girlando, Z.G. Soos, Chem. Phys. Lett. **369**, 428 (2003).
  - <sup>14</sup> M. Masino, A. Girlando, A. Brillante, R.G. Della Valle, E. Venuti, N. Drichko, M. Dressel, Chem. Phys. **325**, 71 (2006).
  - <sup>15</sup> C. Katan, P. E. Blöchl, P. Margl, C. Koenig, Phys. Rev. B **53**, 12112 (1996).
  - <sup>16</sup> P. Ranzieri, M. Masino and A. Girlando, unpublished.
  - <sup>17</sup> A. Painelli, L. Del Freato, Z. G. Soos, Synth. Metals **133-134**, 619 (2003). and references therein.
  - <sup>18</sup> Z. G. Soos, S. A. Bewick, A. Peri, A. Painelli, J. Chem. Phys. **120**, 6712 (2004)
  - <sup>19</sup> W. K. Kwok, U. Welp, K. D. Carlson, G. W. Crabtree, K. G. Vandervoort, H. H. Wang, A. M. Kini, J. M. Williams, D. L. Stupka, L. K. Montgomery, J. E. Thompson, Phys. Rev. B **42**, 8686 (1990).
  - <sup>20</sup> V. Oison, P. Rabiller, C. Katan, J. Phys. Chem A **108**, 11049 (2004).
  - <sup>21</sup> S. H. Walmsley, D. P. Craig, *Excitons in Molecular Crystals: Theory and Applications*, Benjamin, New York, 1968.
  - <sup>22</sup> See discussion in Section III A. For parallel polarization we do not have the check by absorbance, as the sample is completely opaque in the parallel polarization.